Bioelectrochemistry 144 (2022) 108038

Contents lists available at ScienceDirect

Bioelectrochemistry

journal homepage: www.elsevier.com/locate/bioelechem

A novel real-time TMAO detection method based on microbial electrochemical technology

Yue Yi [a,b], Axin Liang [a,b], Lin Luo [a,b], Yuxuan Zang [c], Hongyu Zhao [c], Aiqin Luo [a,b,*]

[a] School of Life Science, Beijing Institute of Technology, Beijing 100081, China
[b] Key Laboratory of Molecular Medicine and Biotherapy, Ministry of Industry and Information Technology, Beijing Institute of Technology, Beijing 100081, China
[c] Institute of Environmental Biology and Life Support Technology, School of Biological Science and Medical Engineering, Beihang University, Beijing 100083, China

ARTICLE INFO

Article history:
Received 15 August 2021
Received in revised form 4 December 2021
Accepted 6 December 2021
Available online 8 December 2021

Keywords:
Trimethylamine N-oxide
Electrochemically Active Bacteria
Shewanella loihica PV-4
Extracellular Electron Transfer
Bioelectrochemical System
Biosensor

ABSTRACT

Trimethylamine N-oxide (TMAO) is considered to be a novel biomarker of cardiovascular diseases. However, the traditional TMAO detection method has failed to meet the requirements of real-time and point-of-care tests. Herein, a novel TMAO detection method based on microbial electrochemical technology is established, which realizes the direct conversion of TMAO concentration into electrical signals. Attached *Shewanella loihica* PV-4 was first proven to be capable of simultaneous inward extracellular electron transfer and TMAO reduction. The TMAO detection method showed a wide linear range of 0 to 250 μM, a high sensitivity of 23.92 μA/mM, and a low limit of detection of 5.96 μM. In addition, the TMAO detection process was accomplished within 600 s, with an acceptable accuracy of 90% in the real serum, showing high feasibility in clinical applications.

1. Introduction

Trimethylamine N-oxide (TMAO) is considered to be a critical link between diet and cardiovascular diseases, and there have been extensive studies on the biosynthesis pathway of TMAO and its harmful effects on the cardiovascular system [1–3]. TMAO originates from choline-containing compounds (*e.g.,* in fish, red meat, and eggs), and it is generated from microbiome metabolism in the gut and FMO_3 enzyme catalysis in the liver. An elevated TMAO level in the serum suppresses the reverse transport of cholesterol [4], leads to inflammation and endothelial dysfunction in the arterial wall [5], promotes atherosclerosis, and eventually increases the risks of major adverse cardiovascular events [6,7]. Several clinical cohort studies have proven that the TMAO level can predicted a 5-year mortality risk in stable coronary artery disease [8] and serves as a biomarker of early-stage atherosclerosis [9]. In addition, recent studies have revealed that an increase in TMAO interfered with lipid metabolism and enhanced the hyperreactivity of platelets, which indicated that TMAO is also an independent risk factor for thrombosis and heart failure [10,11]. Therefore, the rapid detection of TMAO has important clinical value for the early diagnosis of cardiovascular diseases.

The commonly used TMAO detection methods mainly include colorimetry and chromatography. The colorimetry method is based on the reduction reaction from TMAO to trimethylamine (TMA) and the colour reaction to quantify reducing agents, which depends on most toxic agents (such as triclosan and titanium trichloride) and tedious operations [12,13]. Additionally, the colorimetry methods are susceptible to the colour of the samples, resulting in relatively low accuracy. Compared with the colorimetry method, the chromatographic method shows higher accuracy and sensitivity. Liquid chromatography with on-line mass spectrometry (LC–MS) is most widely used to investigate the relationships between TMAO and cardiovascular diseases [8,9,14]. Wang et al. determined the level of TMAO in mouse serum with LC–MS and first proved that TMAO promoted atherosclerosis [7]. Other chromatographic methods, including gas chromatography–mass spectrometry [15], ion chromatography [16], fluorescence [17], and capillary electrophoresis [18], were reported for the detection of TMAO with a limit of detection (LOD) ranging from 1.3 μM to 14.9 μM. Nonetheless, chromatographic methods rely on time-consuming preparation processes, expensive equipment, and specialized technicians, which restricts their application in point-of-care testing (POCT).

* Corresponding author at: School of Life, Beijing Institute of Technology, 5 Zhongguancun South Street, Haidian DIST, Beijing 100081, China.
E-mail address: bitluo@bit.edu.cn (A. Luo).

https://doi.org/10.1016/j.bioelechem.2021.108038
1567-5394/

Electrochemical sensors provide an alternative way to realize TMAO-POCT detection. TMAO was detected by measuring the consumption of reducing agents in the process of TMAO reduction to TMA, in which reductase and electrodes were employed to replace toxic reagents in the traditional colorimetry method. Biljana et al. first reported an electrochemical biosensor for TMAO detection with immobilized TMAO reductase (TorA), which realized the direct conversion of TMAO levels to electrical signals [19]. Armel et al. improved the electrochemical biosensor by optimizing the oxygen anti-interference membrane, and the LOD reached 10 μM [20]. However, the immobilized enzyme sensor depended on complex preparation processes (such as enzyme purification and protein reconstruction), and the sensitivity was only 2.75 μA/mM [20], which made it vulnerable to environmental interferences in clinical applications.

Microbial electrochemical technology, the combination of electrochemically active microorganisms (EAMs) and bioelectrochemical systems (BESs), aims to avoid the disadvantages of the complex preparation process and low sensitivity of immobilized enzyme sensors. EAMs are characterized by extracellular electron transfer (EET) [21], where electrons are transferred from the electrodes to the intracellular reductase in an inward pathway [22]. Si et al. first reported a whole-cell electrochemical biosensing system for the fumarate detection and early diagnosis of renal cell carcinoma [23]. The fumarate levels were converted into electrical signals by the model EAM strain *Shewanella oneidensis* MR-1, and the sensitivity reached ~ 250 μA/mM without enzyme purification and immobilization [23]. The sensitive whole-cell amperometric detection of riboflavin was reported with a sensitivity of 4100 μA/mM [24]. Yu et al. recently reported a nitrate detection method using mixed-culture EAMs with a sensitivity of 1970 μA/mM [25]. Therefore, EAMs instead of enzymes improved the detection sensitivity of the electrochemical sensors and simplified the preparation process of the sensors. However, traditional microbial electrochemical sensors are mainly based on EAM biofilms [26,27], which require a time-consuming start-up process (approximately 1–4 weeks) before detection [28], limiting real-time detection. Biofilm formation is a complex process, and the primary step is bacterial cell attachment [29–31]. Some EAM strains (such as *Shewanella oneidensis* MR-1 and *Shewanella loihica* PV-4) have been reported to perform outward EET after cell attachment [32–34]. Therefore, real-time detection can be realized by replacing EAM biofilms with attached EAMs. There have only been studies on the outward EET capacity of attached EAMs [32–34]. TMAO detection is based on the inward EET of EAMs, but the inward EET capacity of the attached EAMs remains to be explored.

Shewanella species are capable of employing TMAO as a terminal electron acceptor for aerobic respiration [35,36]. As a model microorganism, *S. loihica* PV-4 has shown an excellent capacity for inward EET, and extracellular electron transfer was performed by contacting electrodes directly [37,38]. Therefore, *S. loihica* PV-4 may reduce TMAO with extracellular electrons by inward EET, and this is expected to establish a new method for real-time TMAO detection. Herein, the cell attachment process of *S. loihica* PV-4 on electrodes was first investigated by the combination of electrochemical technology and micro-observation. The feasibility of TMAO reduction was revealed by using the attached *S. loihica* PV-4 in a BES, and the electrochemical characteristics of TMAO reduction and electron transfer were determined. The relationship between the TMAO levels and the inward current of *S. loihica* PV-4 was established by spike tests, and the sensitivity and LOD of TMAO detection with attached *S. loihica* PV-4 was quantified. Finally, the feasibility and accuracy of TMAO detection with *S. loihica* PV-4 in clinical applications were tested by taking true serum as an example.

2. Materials and methods

2.1. Microbial cultivation

S. loihica PV-4 (ATCC BAA-1088) was purchased from ATCC and stored at −80 ℃. Luria-Bertani medium, including 10 g/L tryptone, 10 g/L NaCl, and 5 g/L yeast extract, was used to cultivate *S. loihica* PV-4 with an inoculation proportion of 0.1% (v/v). The culture conditions were set as a rotation speed of 150 rpm and temperature of 20 ℃. The suspension was centrifuged by high-speed centrifugation when the growth of *S. loihica* PV-4 entered a platform stage (OD_{600}≈2.0), and then, the pellet was resuspended in the same volume of defined medium (DM) containing 1 g/L $NaHCO_3$, 0.13 g/L KCl, 0.027 g/L $CaCl_2{\cdot}2H_2O$, 0.2 g/L $MgCl_2{\cdot}6H_2O$, 5.85 g/L NaCl, and 7.2 g/L HEPES [37]. Finally, the resulting *S. loihica* PV-4 suspension was used to construct BESs and was restored at 4 ℃ before use.

2.2. Bioelectrochemical systems with attached S. loihica PV-4

Three identical BESs with three-electrode systems were constructed, which contained a piece of 1 cm × 1 cm carbon cloth (WOS1009, CeTech, China) as the working electrode, 1-mm-diameter platinum (Pt210, AiDa, China) wire as the counter electrode, Ag/AgCl electrode (R0303, AiDa, China; 222.4 mV vs. standard hydrogen electrode) as the reference electrode, and a cell with a working volume of 40 mL. Except for Ag/AgCl electrodes, all components of BESs were sterilized by high-temperature steam. Ag/AgCl electrodes were immersed in 75% alcohol overnight before use [39]. All BESs were constructed in a laminar flow cabinet (SW-CJ-1F, Airtech, China). After assembly, all BESs were filled with 40 mL of *S. loihica* PV-4 suspension without the application of constant potential. The open circuit potential of the working electrodes of BESs was recorded *via* a data acquisition system (USB-1608FS, Measurement Computing Corporation, USA) to monitor the cell attachment of *S. loihica* PV-4. The attachment process lasted for 1 h, and the attached *S. loihica* PV-4 in the BES was used for the following experiments. A schematic diagram of *S. lohica* PV-4 cell attachment and TMAO detection is shown in Schematic 1. Electrochemical impedance spectroscopy (EIS) was performed before and after *S. loihica* PV-4 cell attachment to illustrate the change in the electrochemical characteristics. The detailed parameters of the EIS measurement were set as a frequency range of 50 mHz to 100 kHz and a disturbance voltage of 5 mV.

2.3. Micro-observation of attached S. loihica PV-4

After 3600 s of cell attachment, the morphology and viability of the attached *S. loihica* PV-4 in the BES were observed by scanning electron microscopy (SEM) and confocal laser scanning microscopy (CLSM). Sample preparation before SEM observation was performed according to previous studies. First, three 0.2 cm × 0.2 cm pieces of carbon cloth were sampled in each BES. Then, all the samples were soaked in 2.5% glutaraldehyde solution for 3.5 h. After that, the samples were treated with 10%, 25%, 50%, 75%, 90%, and 100% ethyl alcohol, and each treatment lasted 20 min. Finally, the samples were dried and sprayed with gold [40–42]. A LIVE/DEAD BacLight Bacterial Viability Kit (7012, Invitrogen, USA) was used to stain electrode samples before CLSM observation, and the adsorption/emission wavelengths were 480 nm/530 nm and 488 nm/660 nm to distinguish different microbial viabilities.

2.4. Electrochemical characteristics of TMAO reduction

A series of electrochemical experiments were performed to characterize the reduction of TMAO by the attached *S. loihica* PV-

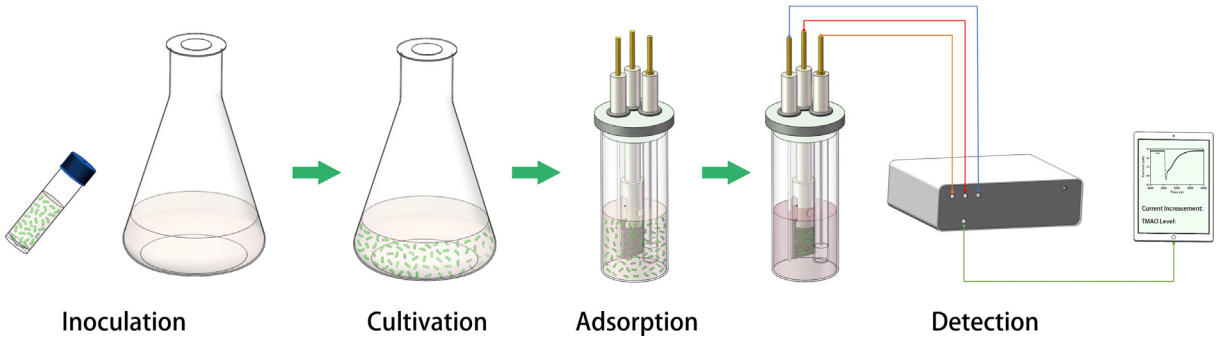

Schematic 1. Schematic diagram of attached *S. lohica* PV-4 preparation and TMAO detection.

4 in the BES. All BESs were refreshed by the anoxic DM supplemented with 5 mM TMAO after 1 h of *S. loihica* PV-4 cell attachment, and the electrolyte was self-circulated to accelerate mass transfer. Chronoamperometry was used to reveal the feasibility of TMAO reduction with the attached *S. loihica* PV-4, and i-t curves were recorded with a frequency of 0.1 Hz and a constant potential of 0 V (vs. reference electrode). With sufficient substrate, cyclic voltammetry (CV) was employed to analyse the onset potential and half-reaction potential of the TMAO bioelectroreduction. When substrate depletion occurred, CV and differential pulse voltammetry (DPV) were used to investigate the electron transfer mechanism [37,38]. CV was performed with the following parameters: initial potential of 0.4 V, quiet time of 30 s, scan range of −0.6 V to 0.4 V, and scan rate of 5 mV/s. The detailed parameters of DPV were set as follows: positive scan from −0.6 V to 0.4 V, negative scan from 0.4 V to −0.6 V, quiet time of 60 s, and scan rate of 1 mV/s.

2.5. TMAO detection

Three BESs with the attached *S. loihica* PV-4 were prepared for TMAO detection. The anaerobic DM containing no TMAO was used to fill the BESs, and the i-t curves were recorded with the same parameters. The baseline was determined when the currents were stable. After that, 0.1 mL of 10 mM TMAO concentrated solution was injected into the BESs, and the current response was then recorded. The final TMAO in the BESs was set from 25 μM to 250 μM by changing the concentration of the TMAO concentrated solution. The selected concentration range was consistent with the TMAO levels in the serum of patients with atherosclerosis and chronic kidney disease [43]. The relationship between the TMAO levels and bioelectrical signals was established by using Prism 8 (GraphPad Software, USA).

The feasibility of TMAO detection with the attached *S. loihica* PV-4 in clinical applications was investigated by replacing DM medium with real serum. Three different TMAO concentrations were detected under the same procedures. The accuracy of the novel method was evaluated by comparing the predicted value of TMAO concentration with the standard addition value.

3. Results and discussion

3.1. Electrochemical and morphological characteristics of attached S. loihica PV-4

Bacterial attachment is the foundation of real-time detection with EAMs as the sensing elements of biosensors. The attachment of the *S. loihica* PV-4 cells on the carbon cloth was evaluated by electrochemical measurements and microscopic examination. As shown in Fig. 1a, the open circuit potential of the working electrodes decreased when the BESs were refreshed with the *S. loihica* PV-4 suspension, and the downwards trend of the potential was repeated among different BESs. There were similar phenomena in our previous study [38], which was due to the accumulation of negatively charged cells [44]. During the cell attachment process, the open circuit potential of the working electrodes became stable (-440.5 ± 26.4 mV) after a decrease, which indicated complete coverage attachment. By analysing the change trends of the potential, the attachment of *S. loihica* PV-4 on the carbon cloth was accomplished at 25%, 50%, 75%, and 100% within 1900 s, 3900 s, 6800 s, and 10,000 s, respectively. Considering the requirement of rapid preparation for real-time detection, 3600 s (close to half the level of complete cell attachment) was chosen as the attachment time for the following experiments.

The cell attachment was further observed by CLSM. Based on different membrane permeabilities, the living bacteria are shown in green, while the dead bacteria are shown in red. Comparing the CLSM images before (Fig. 2a) and after (Fig. 2b) *S. loihica* PV-4 cell attachment, *S. loihica* PV-4 colonized the electrode after 3600 s of attachment and exhibited a high viability, which was further confirmed by SEM images. Single-layer and dispersed *S. loihica* PV-4 cells were observed on the electrode surface (Fig. 2c-f). Compared with biofilms, the attached bacteria did not aggregate [39,45,46], which was conducive to the sensing process. The electrochemical characteristics of the charge transfer resistance (a semicircle in EIS) were observed after cell attachment [31,41,47] (Fig. 1b), which indicated that attached *S. loihica* PV-4 may be electrochemically active. The cells were mainly in direct contact with the electrode, and it was speculated that the inward EET mechanism of attached *S. loihica* PV-4 may be direct electron transfer. Previous studies only reported the inward EET capacity and electron transfer mechanism of *S. loihica* PV-4 biofilms [37,38,48]. The specific electrochemical activity and inward EET pathways of the attached *S. loihica* PV-4 remain to be revealed in the following experiments.

3.2. TMAO electroreduction with attached S. loihica PV-4

A series of electrochemical techniques were employed to evaluate the bioelectroreduction of TMAO. As shown in Fig. 3a, all BESs generated significant inward currents after adding 5 mM TMAO. The current trend exhibited a classical inverted U-shape with TMAO consumption, and the maximum inward current was −34.3 ± 1.7 μA. Previous studies only reported the inward EET capacity of *S. loihica* PV-4 with nitrate and fumarate as the electron acceptor [37,38,48]. The study first revealed that *S. loihica* PV-4 performed inward EET by reducing TMAO. The onset potential of TMAO was approximately −139 ± 23 mV according to the turnover CV (Fig. 3b), which was between the reported onset potentials of nitrate (-100 mV) and fumarate (-250 mV) reduction with *S. loihica*

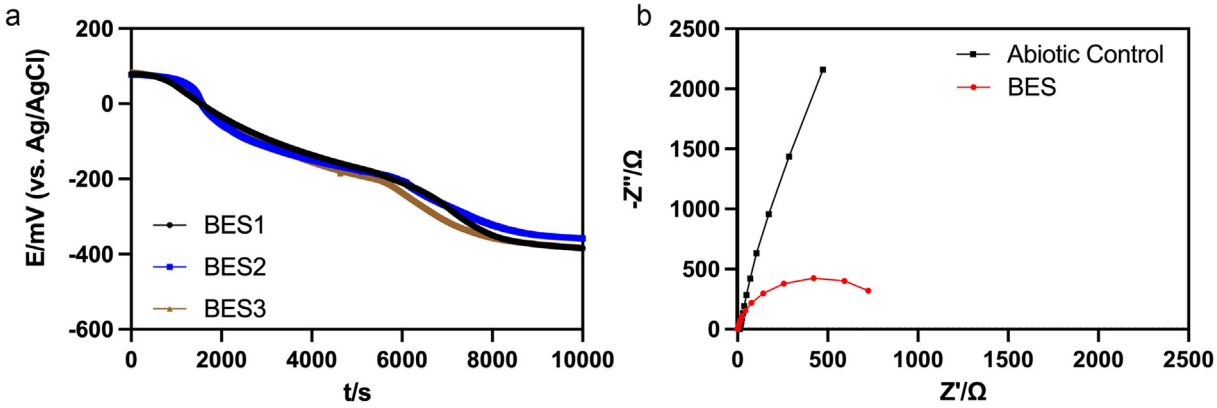

Fig. 1. Electrochemical characteristics of *S. loihica* PV-4 cell attachment.

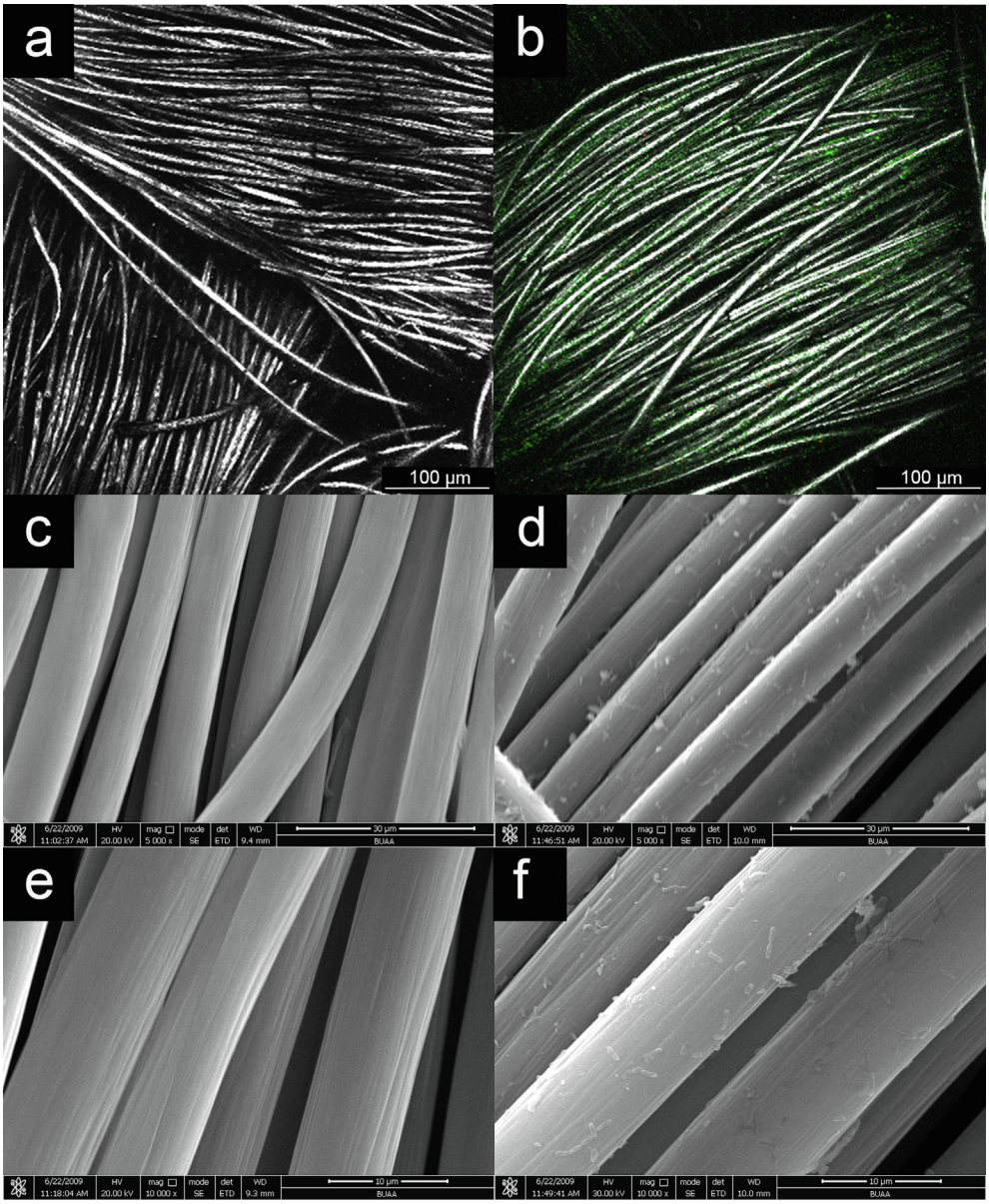

Fig. 2. Morphology and viability of attached *S. loihica* PV-4.

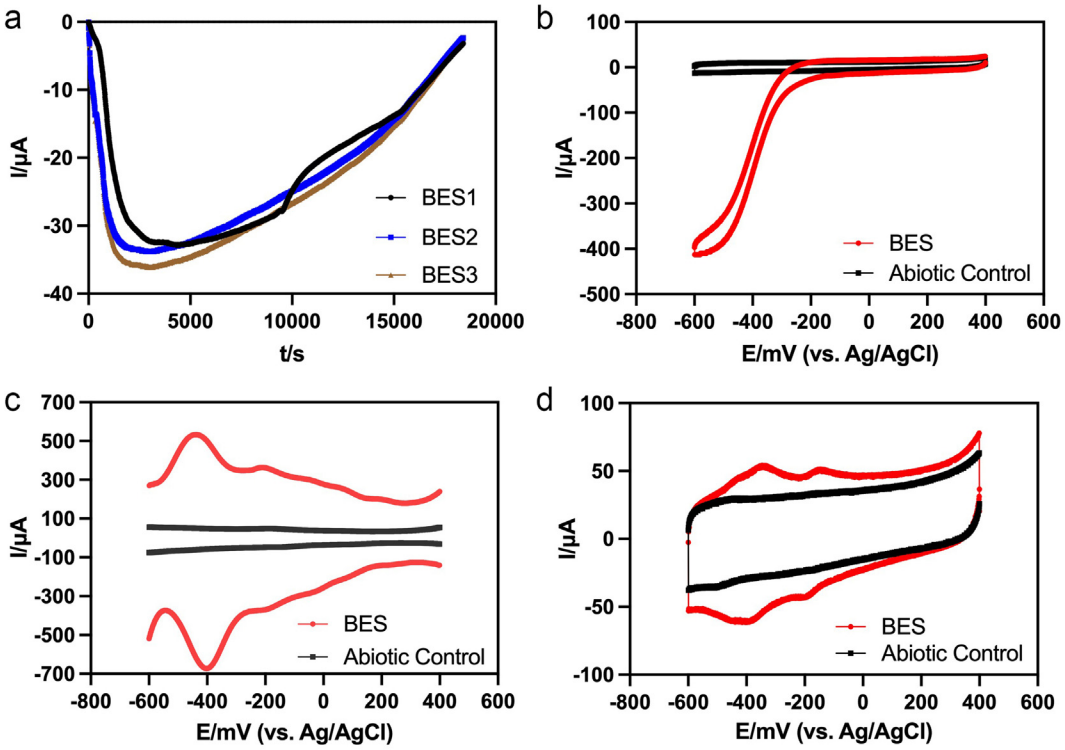

Fig. 3. Electrochemical characteristics of TMAO reduction with attached *S. loihica* PV-4.

PV-4 biofilms [37,38]. In addition, the polarization control was changed to diffusion control with a decrease in the applied potential, and the half-wave potential of the TMAO reduction was approximately −400 mV.

The redox components of inward EET were further revealed. The combination of electrochemical techniques, nonturnover CV and DPV, confirmed that two redox systems (E_1 and E_2) were involved in the extracellular electron transfer of the TMAO bioelectroreduction (Fig. 3c-d). The mid-term potential of E_1 was −418 ± 7 mV, which was consistent with the value of bound riboflavin (-400 mV) [38,49], suggesting that direct electron transfer was involved in the inward EET of attached *S. loihica* PV-4. E_2 with a mid-term potential of −202 ± 5 mV was also observed in previous studies, which was supposed to represent outer membrane cytochrome *c* [50] and presented a surface-controlled redox reaction [38]. Based on the above results, the attached *S. loihica* PV-4 in the BES performed inward EET and TMAO reduction simultaneously, which provided a basis for the real-time detection of TMAO.

3.3. TMAO detection with attached S. loihica PV-4

TMAO at different concentrations was tested to reveal the relationship between the inward currents and TMAO levels. There were low background currents without TMAO addition in Fig. 4a. The currents showed a slight fluctuation, indicating a stable baseline of TMAO detection. When 25 μM TMAO was added, the inward currents increased sharply, with a peak of −1.60 ± 0.19 μA. The currents returned to baseline again after 600 s of reaction, suggesting the depletion of TMAO. There were rapid responses and high peak currents in previous studies on fumarate and nitrate detection with EAMs [23,25], which were considered competitive advantages of microbial electrochemical technology.

Table 1
Detailed current responses with different TMAO levels.

TMAO concentration (μM)	Maximum current (μA)	Current delta (μA)
0	−0.50 ± 0.08	/
25	−1.60 ± 0.19	1.1 ± 0.13
50	−2.05 ± 0.09	1.55 ± 0.07
75	−2.51 ± 0.11	2.01 ± 0.05
100	−3.21 ± 0.17	2.71 ± 0.13
125	−3.71 ± 0.24	3.21 ± 0.19
150	−4.29 ± 0.26	3.79 ± 0.25
200	−5.65 ± 0.18	5.15 ± 0.16
250	−6.66 ± 0.38	6.16 ± 0.33

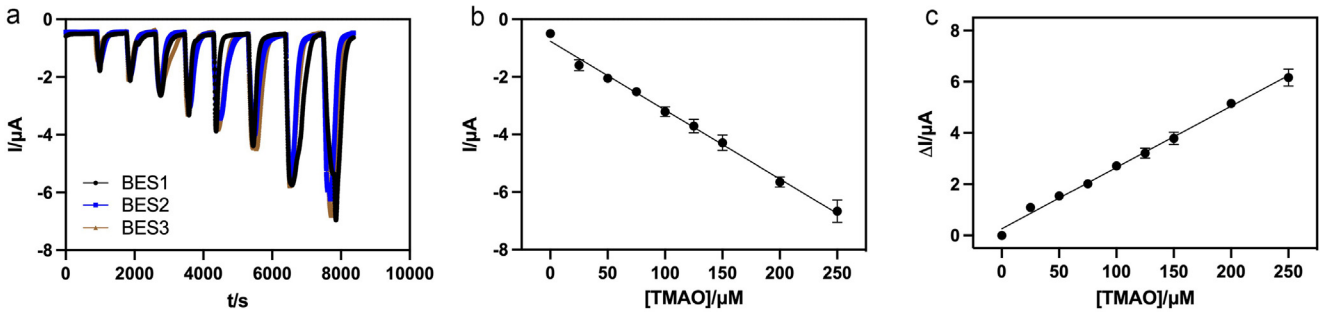

Fig. 4. TMAO reduction with attached *S. loihica* PV-4.

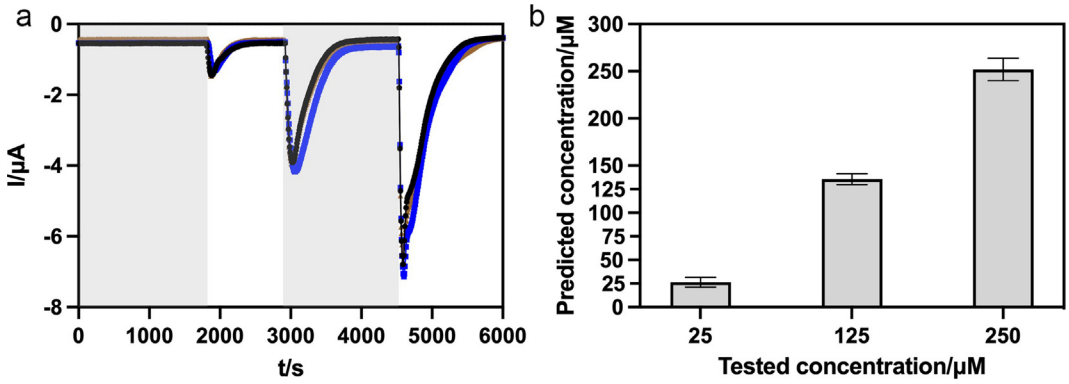

Fig. 5. TMAO detection with attached *S. loihica* PV-4 by using real serum.

The peak values of the inward currents increased correspondingly with increasing TMAO levels. Detailed responses of the inward currents are shown in Table 1, and a good linear relationship was found between the TMAO concentrations and the maximum *S. loihica* PV-4 inward currents (R^2 = 0.986, Fig. 4b). The reaction time of the TMAO reduction was prolonged with the increase in TMAO levels (from ~ 450 s to ~ 900 s), which conformed to Faraday's law. Previous studies showed that two electrical signals were positively correlated with substrate concentration [51–53]. The most widely used one was the total amount of electron transfer during the polarization process [52,53], and the other was the current delta after substrate addition [24,25]. Considering the requirements of the POCT tests for a high signal-to-noise (S/N) ratio and short detection time, the current delta after TMAO addition was used to establish the relationship between the inward currents of attached *S. loihica* PV-4 and TMAO levels (Fig. 4c) as follows:

$$y = 0.02392x + 0.2625, \quad (1)$$

where x represents the TMAO level (μM) and y refers to the increase in the inward currents (μA). The determination coefficient of the model reached 0.989, indicating that the TMAO levels were fully explained by the current delta. Based on the model, the sensitivity of TMAO detection with attached *S. loihica* PV-4 was 23.92 μA/mM, which was almost 10 times that of the reported electrochemical sensors for TMAO detection [20]. In addition, the key element of TMAO detection was whole cells in the study, which omitted enzyme purification and protein reconstruction. The LOD was calculated as 5.96 μM with an S/N ratio of 3, which was comparable to that of chromatography for TMAO detection [15–18]. The method was performed without complex sample preparation, expensive equipment, and professional technicians, showing great prospects in clinical applications.

The feasibility of TMAO detection with absorbed *S. loihica* PV-4 in clinical applications remains to be explored due to the complex components of real serum. There were similar background currents with slight fluctuations when using real calf serum to replace DM (Fig. 5a). Notably, after adding the specific TMAO, the inward currents increased as expected (Fig. 5a), suggesting that the real serum did not contain electroactive material or available electron acceptors. The current deltas were 0.89 ± 0.13 μA (25 μM), 3.51 ± 0.14 μA (125 μM), and 6.29 ± 0.28 μA (250 μM), which were basically the same as the results shown in Fig. 4c. According to the obtained current deltas, the TMAO levels of the different samples were predicted by Eq. (1), and there was a less than 9% difference between the real and predicted TMAO levels (Fig. 5b), indicating that attached *S. loihica* PV-4 accurately detected the TMAO levels in the real serum.

In conclusion, a novel TMAO detection method based on attached *S. lohica* PV-4 was established, which provided novel insight into real-time and POCT tests. Compared with chromatography and enzyme electrochemical sensors, the method exhibited higher sensitivity and low LOD with only simple sample treatment and sensor preparation, which largely reduced the detection time and cost. Nonetheless, the milliliter-sized BESs in the study were used to demonstrate the feasibility of TMAO reduction with attached *S. loihica* PV-4, which remained to be further miniaturized in practical applications. Therefore, future studies will focus on the miniaturization and robotization of the method. For example, the sample volume of TMAO detection can be reduced to less than 10 μL by combining the method with screen-printed electrodes [54], and the method can also be improved with paper-based microfluidic devices to realize TMAO real-time detection without external energy input [55].

4. Conclusion

In summary, *S. loihica* PV-4 was first reported to perform inward EET with TMAO as the electron acceptor. In the absence of a mature biofilm, simultaneous TMAO reduction and inward EET were realized only after the attachment of *S. loihica* PV-4 cells on electrodes. The delta value of the *S. loihica* PV-4 inward current was linearly related to TMAO levels in the range of 0–250 μM. The novel TMAO detection method was established based on this characteristic, which exhibited a high sensitivity of 23.92 μA/mM and low LOD of 5.96 μM, showing great prospects in POCT.

Declaration of Competing Interest

The authors declare that they have no known competing financial interests or personal relationships that could have appeared to influence the work reported in this paper.

Acknowledgements

This work was financially supported by grants from the Beijing Institute of Technology Research Fund Program for Young Scholars [3160011182123], China Postdoctoral Science Foundation [2020 M670099], and the Fundamental Research Funds for the Central Universities.

Appendix A. Supplementary material

Supplementary data to this article can be found online at https://doi.org/10.1016/j.bioelechem.2021.108038.

References

[1] C.E. Cho, M.A. Caudill, Trimethylamine-N-Oxide: Friend, foe, or simply caught in the cross-fire, Trends Endocrinol. Metab. 28 (2) (2017) 121–130.

[2] A. Nowiński, M. Ufnal, Trimethylamine N-oxide: A harmful, protective or diagnostic marker in lifestyle diseases, Nutrition 46 (2018) 7–12.

[3] W.H.W. Tang, D.Y. Li, S.L. Hazen, Dietary metabolism, the gut microbiome, and heart failure, Nat. Rev. Cardiol. 16 (2019) 137–154.

[4] R.A. Koeth, Z. Wang, B.S. Levison, J.A. Buffa, E. Org, B.T. Sheehy, E.B. Britt, X. Fu, Y. Wu, L. Li, J.D. Smith, J.A. DiDonato, J. Chen, H. Li, G.D. Wu, J.D. Lewis, M. Warrier, J.M. Brown, R.M. Krauss, W.H.W. Tang, F.D. Bushman, A.J. Lusis, S.L. Hazen, Intestinal microbiota metabolism of l-carnitine, a nutrient in red meat, promotes atherosclerosis, Nat. Med. 19 (2013) 576–585.

[5] X. Sun, X. Jiao, Y. Ma, Y. Liu, L. Zhang, Y. He, Y. Chen, Trimethylamine N-oxide induces inflammation and endothelial dysfunction in human umbilical vein endothelial cells via activating ROS-TXNIP-NLRP3 inflammasome, Biochem. Biophys. Res. Commun. 481 (2016) 63–70.

[6] W.H. Tang, Z. Wang, B.S. Levison, Intestinal microbial metabolism of phosphatidylcholine and cardiovascular risk, J. Vasc. Surg. 58 (2013) 549.

[7] Z. Wang, E. Klipfell, B.J. Bennett, R. Koeth, B.S. Levison, B. DuGar, A.E. Feldstein, E.B. Britt, X. Fu, Y.M. Chung, Y. Wu, P. Schauer, J.D. Smith, H. Allayee, W.H.W. Tang, J.A. DiDonato, A.J. Lusis, S.L. Hazen, Gut flora metabolism of phosphatidylcholine promotes cardiovascular disease, Nature 472 (2011) 57–63.

[8] V. Senthong, Z. Wang, X.S. Li, Y. Fan, Y. Wu, W.H. Wilson Tang, S.L. Hazen, Intestinal microbiota-generated metabolite trimethylamine-n-oxide and 5-year mortality risk in stable coronary artery disease: The contributory role of intestinal microbiota in a courage-like patient cohort, J. Am. Heart Assoc. 5 (6) (2016), https://doi.org/10.1161/JAHA.115.002816.

[9] E. Randrianarisoa, A. Lehn-Stefan, X. Wang, M. Hoene, A. Peter, S.S. Heinzmann, X. Zhao, I. Königsrainer, A. Königsrainer, B. Balletshofer, J. Machann, F. Schick, A. Fritsche, H.-U. Häring, G. Xu, R. Lehmann, N. Stefan, Relationship of serum trimethylamine N-oxide (TMAO) levels with early atherosclerosis in humans, Sci. Rep. 6 (2016) 26745.

[10] M. Makrecka-Kuka, K. Volska, U. Antone, R. Vilskersts, S. Grinberga, D. Bandere, E. Liepinsh, M. Dambrova, Trimethylamine N-oxide impairs pyruvate and fatty acid oxidation in cardiac mitochondria, Toxicol. Lett. 267 (2017) 32–38.

[11] W. Zhu, J.C. Gregory, E. Org, J.A. Buffa, N. Gupta, Z. Wang, L. Li, X. Fu, Y. Wu, M. Mehrabian, R.B. Sartor, T.M. McIntyre, R.L. Silverstein, W.H.W. Tang, J.A. DiDonato, J.M. Brown, A.J. Lusis, S.L. Hazen, Gut microbial metabolite TMAO enhances platelet hyperreactivity and thrombosis risk, Cell 165 (2016) 111–124.

[12] A.B. Bockus, B.A. Seibel, Trimethylamine oxide accumulation as a function of depth in Hawaiian mid-water fishes, Deep-Sea Res. Pt. I (112) (2016) 37–44.

[13] S.W. Gibb, A.D. Hatton, The occurrence and distribution of trimethylamine-N-oxide in Antarctic coastal waters, Mar. Chem. 91 (2004) 65–75.

[14] X.S. Li, S. Obeid, R. Klingenberg, B. Gencer, F. Mach, L. Räber, S. Windecker, N. Rodondi, D. Nanchen, O. Muller, M.X. Miranda, C.M. Matter, Y. Wu, L. Li, Z. Wang, H.S. Alamri, V. Gogonea, Y.M. Chung, W.H.W. Tang, S.L. Hazen, T.F. Lüscher, Gut microbiota-dependent trimethylamine N-oxide in acute coronary syndromes: a prognostic marker for incident cardiovascular events beyond traditional risk factors, Eur. Heart J. 38 (2017) 814–824.

[15] G.A. Mills, V. Walker, H. Mughal, Quantitative determination of trimethylamine in urine by solid-phase microextraction and gas chromatography-mass spectrometry, J. Chromatogr. B: Biomed. Sci. Appl. 723 (1-2) (1999) 281–285.

[16] F. Li, H.-Y. Liu, C.-h. Xue, X.-Q. Xin, J. Xu, Y.-G. Chang, Y. Xue, L.-A. Yin, Simultaneous determination of dimethylamine, trimethylamine and trimethylamine-n-oxide in aquatic products extracts by ion chromatography with non-suppressed conductivity detection, J. Chromatogr. A 1216 (31) (2009) 5924–5926.

[17] H. Yu, W.-C. Geng, Z. Zheng, J. Gao, D.-S. Guo, Y. Wang, Facile fluorescence monitoring of gut microbial metabolite trimethylamine N-oxide via molecular recognition of guanidinium-modified calixarene, Theranostics 9 (16) (2019) 4624–4632.

[18] M. Timm, B.M. Jørgensen, Simultaneous determination of ammonia, dimethylamine, trimethylamine and trimethylamine-n-oxide in fish extracts by capillary electrophoresis with indirect UV-detection, Food Chem. 76 (4) (2002) 509–518.

[19] B. Mitrova, A.F.T. Waffo, P. Kaufmann, C. Iobbi-Nivol, S. Leimkühler, U. Wollenberger, Trimethylamine N-oxide electrochemical biosensor with a chimeric enzyme, ChemElectroChem 6 (6) (2019) 1732–1737.

[20] A.F.T. Waffo, B. Mitrova, K. Tiedemann, C. Iobbi-Nivol, S. Leimkühler, U. Wollenberger, Electrochemical trimethylamine N-oxide biosensor with enzyme-based oxygen-scavenging membrane for long-term operation under ambient air, Biosensors-Basel 11 (4) (2021) 98, https://doi.org/10.3390/bios11040098.

[21] B.E. Logan, Exoelectrogenic bacteria that power microbial fuel cells, Nat. Rev. Microbiol. 7 (5) (2009) 375–381.

[22] Y. Jiang, R.J. Zeng, Bidirectional extracellular electron transfers of electrode-biofilm: Mechanism and application, Bioresour. Technol. 271 (2019) 439–448.

[23] R.-W. Si, D.-D. Zhai, Z.-H. Liao, L.u. Gao, Y.-C. Yong, A whole-cell electrochemical biosensing system based on bacterial inward electron flow for fumarate quantification, Biosens. Bioelectron. 68 (2015) 34–40.

[24] R.-W. Si, Y. Yang, Y.-Y. Yu, S. Han, C.-L. Zhang, D.-Z. Sun, D.-D. Zhai, X. Liu, Y.-C. Yong, Wiring bacterial electron flow for sensitive whole-cell amperometric detection of riboflavin, Anal. Chem. 88 (22) (2016) 11222–11228.

[25] Y.-Y. Yu, X.-L. Ding, W.-Z. Quan, Q. Niu, Z. Fang, M.F. Dapaah, T. You, X. Xiao, L. Cheng, Dynamically controlling the electrode potential of a microbial fuel cell-powered biocathode for sensitive quantification of nitrate, Electrochim. Acta 369 (2021) 137661, https://doi.org/10.1016/j.electacta.2020.137661.

[26] N.a. Chu, Q. Liang, W. Hao, Y. Jiang, P. Liang, R.J. Zeng, Microbial electrochemical sensor for water biotoxicity monitoring, Chem. Eng. J. 404 (2021) 127053, https://doi.org/10.1016/j.cej.2020.127053.

[27] X. Qi, S. Wang, T. Li, X. Wang, Y. Jiang, Y. Zhou, X. Zhou, X. Huang, P. Liang, An electroactive biofilm-based biosensor for water safety: Pollutants detection and early-warning, Biosen. Bioelectron. 173 (2021) 112822, https://doi.org/10.1016/j.bios.2020.112822.

[28] G. Liu, M.D. Yates, S. Cheng, D.F. Call, D. Sun, B.E. Logan, Examination of microbial fuel cell start-up times with domestic wastewater and additional amendments, Bioresour. Technol. 102 (15) (2011) 7301–7306.

[29] X. Fan, Y. Zhou, X. Jin, R.-B. Song, Z. Li, Q. Zhang, Carbon material-based anodes in the microbial fuel cells, Carbon, Energy 3 (3) (2021) 449–472.

[30] H.-C. Flemming, S. Wuertz, Bacteria and archaea on Earth and their abundance in biofilms, Nat. Rev. Microbiol. 17 (4) (2019) 247–260.

[31] S.E. Astorga, L.X. Hu, E. Marsili, Y.Z. Huang, Ordered micropillar array gold electrode increases electrochemical signature of early biofilm attachment, Mater. Des. 185 (2020) 108256.

[32] G.J. Newton, S. Mori, R. Nakamura, K. Hashimoto, K. Watanabe, Analyses of current-generating mechanisms of Shewanella loihica PV-4 and Shewanella oneidensis MR-1 in microbial fuel cells, Appl. Environ. Microbiol. 75 (2009) 7674–7681.

[33] Y. Yang, Y.Z. Wang, Z. Fang, Y.Y. Yu, Y.C. Yong, Bioelectrochemical biosensor for water toxicity detection: Generation of dual signals for electrochemical assay confirmation, Anal. Bioanal. Chem. 410 (2018) 1231–1236.

[34] Y. Zang, T. Zhao, B. Xie, Y. Feng, Y. Yi, H. Liu, A bio-electrochemical sensor based on suspended Shewanella oneidensis MR-1 for the sensitive assessment of water biotoxicity, Sensor. Actuat. B-Chem. 341 (2021) 130004.

[35] J. Debevere, F. Devlieghere, P. van Sprundel, B. De Meulenaer, Influence of acetate and CO_2 on the TMAO-reduction reaction by Shewanella baltica, Int. J. Food Microbiol. 68 (2001) 115–123.

[36] O.N. Lemaire, F.A. Honore, C. Jourlin-Castelli, V. Mejean, M. Fons, C. Iobbi-Nivol, Efficient respiration on TMAO requires TorD and TorE auxiliary proteins in Shewanella oneidensis, Res. Microbiol. 167 (2016) 630–637.

[37] Y. Yi, T. Zhao, B. Xie, Y. Zang, H. Liu, Dual detection of biochemical oxygen demand and nitrate in water based on bidirectional Shewanella loihica electron transfer, Bioresour. Technol. 309 (2020) 123402.

[38] Y. Yi, T. Zhao, Y. Zang, B. Xie, H. Liu, Different mechanisms for riboflavin to improve the outward and inward extracellular electron transfer of Shewanella loihica, Electrochem. Commun. 124 (2021) 106966.

[39] D. Sun, S.A. Cheng, A.J. Wang, F.J. Li, B.E. Logan, K.F. Cen, Temporal-spatial changes in viabilities and electrochemical properties of anode biofilms, Environ. Sci. Technol. 49 (2015) 5227–5235.

[40] B.Z. Xie, B.J. Liu, Y. Yi, L.G. Yang, D.W. Liang, Y. Zhu, H. Liu, Microbiological mechanism of the improved nitrogen and phosphorus removal by embedding microbial fuel cell in Anaerobic-Anoxic-Oxic wastewater treatment process, Bioresour. Technol. 207 (2016) 109–117.

[41] C.-e. Zhao, J. Wu, S. Kjelleberg, J.S.C. Loo, Q. Zhang, Employing a flexible and low-cost polypyrrole nanotube membrane as an anode to enhance current generation in microbial fuel cells, Small 11 (28) (2015) 3440–3443.

[42] V.B. Wang, J. Du, X. Chen, A.W. Thomas, N.D. Kirchhofer, L.E. Garner, M.T. Maw, W.H. Poh, J. Hinks, S. Wuertz, S. Kjelleberg, Q. Zhang, J.S.C. Loo, G.C. Bazan, Improving charge collection in Escherichia coli-carbon electrode devices with conjugated oligoelectrolytes, Phys. Chem. Chem. Phys. 15 (16) (2013) 5867, https://doi.org/10.1039/c3cp50437a.

[43] J.R. Stubbs, J.A. House, A.J. Ocque, S. Zhang, C. Johnson, C. Kimber, K. Schmidt, A. Gupta, J.B. Wetmore, T.D. Nolin, J.A. Spertus, A.S. Yu, Serum trimethylamine-N-oxide is elevated in CKD and correlates with coronary atherosclerosis burden, J. Am. Soc. Nephrol. 27 (1) (2016) 305–313.

[44] Z. Ning, R. Li, K. Lian, P. Liao, H. Liao, C. Liu, Transport and retention of Shewanella oneidensis strain MR1 in water-saturated porous media with different grain-surface properties, Chemosphere 233 (2019) 57–66.

[45] T. Li, X. Wang, L. Zhou, J. An, J. Li, N. Li, H. Sun, Q. Zhou, Bioelectrochemical sensor using living biofilm to in situ evaluate flocculant toxicity, ACS Sens. 1 (11) (2016) 1374–1379.

[46] S.T. Read, P. Dutta, P.L. Bond, J. Keller, K. Rabaey, Initial development and structure of biofilms on microbial fuel cell anodes, BMC microbiol. 10 (2010) 98.

[47] M. Sindhuja, N.S. Kumar, V. Sudha, S. Harinipriya, Equivalent circuit modeling of microbial fuel cells using impedance spectroscopy, J. Energy Storage 7 (2016) 136–146.

[48] D.i. Suo, Z. Fang, Y.-Y. Yu, Y.-C. Yong, Synthetic curli enables efficient microbial electrocatalysis with stainless-steel electrode, AIChE J. 66 (4) (2020), https://doi.org/10.1002/aic.v66.410.1002/aic.16897.

[49] A. Okamoto, K. Hashimoto, K.H. Nealson, R. Nakamura, Rate enhancement of bacterial extracellular electron transport involves bound flavin semiquinones, Proc. Natl. Acad. Sci. U. S. A. 110 (19) (2013) 7856–7861.

[50] A. Okamoto, R. Nakamura, K. Ishii, K. Hashimoto, In vivo electrochemistry of C-type cytochrome-mediated electron-transfer with chemical marking, ChemBioChem 10 (2009) 2329–2332.

[51] M. Di Lorenzo, T.P. Curtis, I.M. Head, K. Scott, A single-chamber microbial fuel cell as a biosensor for wastewaters, Water Res. 43 (13) (2009) 3145–3154.
[52] Y. Gao, F. Yin, W. Ma, S. Wang, Y. Liu, H. Liu, Rapid detection of biodegradable organic matter in polluted water with microbial fuel cell sensor: Method of partial coulombic yield, Bioelectrochemistry 133 (2020) 107488, https://doi.org/10.1016/j.bioelechem.2020.107488.
[53] M. Kim, S.M. Youn, S.H. Shin, J.G. Jang, S.H. Han, M.S. Hyun, G.M. Gadd, H.J. Kim, Practical field application of a novel BOD monitoring system, J. Environ. Monit. 5 (4) (2003) 640, https://doi.org/10.1039/b304583h.
[54] A.G. Ayankojo, J. Reut, A. Öpik, V. Syritski, Sulfamethizole-imprinted polymer on screen-printed electrodes: Towards the design of a portable environmental sensor, Sensor. Actuat. B-Chem. 320 (2020) 128600, https://doi.org/10.1016/j.snb.2020.128600.
[55] C.-C. Tseng, C.-T. Kung, R.-F. Chen, M.-H. Tsai, H.-R. Chao, Y.-N. Wang, L.-M. Fu, Recent advances in microfluidic paper-based assay devices for diagnosis of human diseases using saliva, tears and sweat samples, Sensor. Actuat. B-Chem. 342 (2021) 130078, https://doi.org/10.1016/j.snb.2021.130078.